Dual-Stage Bifurcation With Genetic Algorithm Extraction for Robust Anti-Antiforensic Steganalysis in Grayscale Images

Yudi Prayudi[1*], Amadeus Pondera Purnacandra[2]

[1,2] *Center for Digital Forensics Studies, Dep Of Informatics, Universitas Islam Indonesia, Indonesia*

*corr-author: prayudi@uii.ac.id

Abstract - Steganalysis plays a crucial role in digital forensics by detecting and retrieving hidden information embedded within digital media. Traditional statistical methods, such as Chi-Square and RS-Analysis, are computationally efficient but ineffective against adaptive steganography techniques that minimize detectable distortions. While recent deep learning-based approaches, particularly Convolutional Neural Networks (CNNs), have improved detection accuracy, most rely on single-stream architectures and focus solely on classification, neglecting the recovery of concealed payloads. This study proposes a dual-stage steganalysis framework that integrates a bifurcated CNN for enhanced detection with a genetic algorithm-based extraction pipeline for payload recovery. The bifurcation architecture extends GBRAS-Net by enabling parallel feature learning paths to capture diverse noise patterns, while the extraction module employs chromosome key encoding, Hilbert Curve scrambling, and LZMA compression to reconstruct hidden data. Evaluations on BOSSbase 1.01 and BOWS 2 datasets show that the proposed method achieves an average detection accuracy of 92.53%, outperforming the original GBRAS-Net (89.8%) and other CNN-based models by a statistically significant margin ($p < 0.01$). Furthermore, the extraction module achieves 100% payload recovery with perfect data integrity verification. The results demonstrate that integrating bifurcated feature learning with robust extraction addresses critical gaps in current steganalysis, offering a practical forensic tool for both detection and reconstruction of hidden information. This approach has significant potential for applications in law enforcement, cybersecurity, and intelligence operations.

Keywords: Steganalysis; antiforensics; Convolutional Neural Network; bifurcation; digital forensics; Genetic Algorithm.

I. INTRODUCTION

Recent advancements in steganographic techniques have introduced substantial challenges to digital forensic investigations. Modern embedding schemes, particularly those driven by AI and evolutionary algorithms, and will produce pixel modifications that resemble natural noise, making traditional statistical detection methods unreliable. Although CNN-based approaches offer improved accuracy, most rely on a single-path architecture and lack payload recovery mechanisms. This study proposes a dual-stage framework combining a bifurcated CNN for enhanced detection with a genetic algorithm–based payload extraction process, enabling both robust classification and complete reconstruction of hidden data.

Digital forensics plays a crucial role in identifying, preserving, and analyzing digital evidence for legal and investigative purposes. However, the rapid evolution of antiforensic techniques, such as steganography, increasingly hinders these efforts. Steganography enables covert communication by embedding hidden messages within seemingly innocuous media files, including images, audio, and video [1, 2]. While the technology itself has legitimate uses, its potential misuse by criminal and terrorist organizations raises significant security concerns [3–5] Traditional steganalysis methods—such as Chi-Square and RS-Analysis—were once effective at detecting early steganographic schemes. However, the emergence of adaptive steganography powered by artificial intelligence and evolutionary algorithms has rendered many of these statistical approaches obsolete [6–9].

More recent research has turned to deep learning, particularly Convolutional Neural Networks (CNNs), for their ability to capture complex spatial patterns and subtle anomalies within images [10–14]. Models such as SRNet, Zhu-Net, and GBRAS-Net have achieved high detection accuracies, yet they still face two major challenges:

1) Overfitting and limited generalization when trained on constrained datasets.

2) Lack of payload recovery capability, which limits their utility in forensic contexts where content retrieval is as critical as detection.

Existing literature largely focuses on detection as the final goal, with minimal attention to payload extraction. This creates a *gap* between identifying the presence of hidden data and producing usable evidence for legal proceedings. Moreover, most CNN-based models employ single-stream architectures, which may be insufficient for learning the complex and diverse noise patterns introduced by modern adaptive steganography.

To address these challenges, we propose a dual-stage bifurcation-enhanced CNN framework based on GBRAS-Net, designed for both *high-accuracy detection* and *complete payload reconstruction*. The bifurcated architecture allows parallel feature extraction from different noise perspectives, improving robustness against sophisticated antiforensic strategies. The extraction stage incorporates a genetic algorithm to encode embedding structures, Hilbert Curve [15] scrambling for spatial distortion resistance, and LZMA [16] compression for data integrity.The contributions of this study are threefold:

1) Novel architecture: Introduction of a bifurcated CNN design tailored for steganalysis in grayscale images, enhancing feature sensitivity.

2) Integrated extraction mechanism: First implementation combining bifurcated CNN detection with genetic algorithm-based payload recovery in a unified forensic framework.

3) Empirical performance: Demonstration of superior detection accuracy (92.53%) and complete payload recovery on benchmark datasets, outperforming traditional and modern steganalysis methods.

By bridging the gap between detection and data recovery, this research advances digital forensic capabilities and offers a practical solution for combating modern antiforensic steganography in real-world investigative scenarios.

II. METHOD

Each input image is first processed with 30 SRM filters[17] to generate a residual tensor. The bifurcated CNN then extracts features through two complementary branches: an ELU [18] branch optimized for low-amplitude noise and a Tanh3 branch tailored for nonlinear distortions. After Global Average Pooling, both feature vectors are concatenated and classified via a softmax layer. During extraction, a 19-bit chromosome encodes embedding parameters, while Hilbert Curve traversal preserves spatial locality to support accurate payload reconstruction.

The distinction between the original GBRAS-Net and the proposed GBRAS-Bifurcated model is presented more specifically and explicitly in

TABLE I. The proposed method extends the GBRAS-Net architecture by introducing a bifurcated convolutional pathway to enhance feature diversity and improve steganalysis performance in grayscale images. The framework operates in two stages: the first stage performs detection using a bifurcated CNN designed to capture complex spatial noise patterns, while the second stage executes payload extraction using a genetic algorithm-based mechanism integrated with Hilbert Curve scrambling and LZMA compression. This dual-stage design allows the system to not only identify stego images with high accuracy but also to recover hidden payloads with robustness against spatial distortion and redundancy.

Two publicly available datasets, BOSSbase 1.01 [19] shown on Fig. 1 and BOWS 2 on Fig. 2, were used for training and evaluation. Both contain 10,000 grayscale images with original dimensions of 512×512 pixels. Prior to training, the images were resized to 256×256 and 512×512 pixels, normalized to intensity values within [0, 1], and augmented using horizontal flipping and random cropping to reduce overfitting and improve generalization. The datasets were split into 70% training, 10% validation, and 20% testing subsets.

In the detection stage, each input image was first processed with 30 Spatial Rich Model (SRM) Fig. 4 filters to highlight high-frequency noise features. The resulting feature maps were then fed into a bifurcated CNN consisting of two parallel convolutional branches. The first branch used the Exponential Linear Unit (ELU) Equation 1 activation to promote smoother gradient propagation, while the second employed the Tanh3 Equation 2 activation to enhance non-linearity and capture distinct feature variations. Each branch incorporated Batch Normalization and Global Average Pooling (GAP) before their outputs were concatenated and passed through fully connected layers. The final classification layer applied a softmax activation to produce binary output (cover or stego). The model was trained using the Adam optimizer with an initial learning rate of 0.001, decaying by a factor of 0.1 every 10 epochs, a batch size of 32, and categorical cross-entropy loss over 50 epochs.

TABLE I
COMPARISON

Aspect	GBRAS-Bifurcated	GBRAS-Net
Architecture	Dual-path (non-trainable + trainable layers)	Single-path (non-trainable SRM filters)
First Layer	Combination of fixed and trainable features	Fixed SRM filters only
Activation Function	3×Tanh	3×Tanh
Generalization	High (adaptive to new data)	Moderate (fixed SRM limits adaptation)
Training Time	Longer	Shorter

The extraction stage was designed to recover hidden payloads from detected stego images. A 19-bit chromosome key TABLE II encoded the payload embedding parameters, including X/Y coordinates, inversion flags, spatial direction, and a decompression indicator. The genetic algorithm guided the search for optimal extraction parameters. To enhance resilience against spatial distortions, pixel positions were permuted using Hilbert Curve transformations in both 4×4 and 8×8 configurations (see Fig. 5 and Fig. 6). The recovered bitstream was compressed and decompressed using LZMA to remove redundancy and verify data integrity. The correctness of the recovered payload was confirmed through MD5 hash comparison with the original embedded data shown on Fig. 7.

The evaluation employed detection accuracy as the primary metric, defined as the proportion of correctly classified cover and stego images, and payload recovery rate as the percentage of bits retrieved without error. Baseline comparisons included statistical methods such as Chi-Square [8] and RS-Analysis [20] as well as deep learning models including SRNet[21], Shi X [22] and GBRAS-Net [23]. To assess statistical significance, paired t-tests were conducted between the proposed method and each baseline, with a significance threshold set at $p < 0.01$.

The entire implementation was conducted on a workstation equipped with an Intel Core i7-12700H CPU, 16 GB RAM, and an NVIDIA RTX 3060 GPU, using Python 3.9 with TensorFlow 2.x as the backend, alongside CUDA 11.x and cuDNN 8.x for GPU acceleration. For reproducibility, random seeds were fixed across NumPy and TensorFlow, and the dataset splits as well as the preprocessing scripts are available upon request. For the hyper-parameters of the GBRAS-Bifurcated model, the network was trained using a batch size of 32 and required 1000 epochs to converge for a specific payload configuration. The Adam optimizer was employed with a learning rate of 0.001, $\beta_1 = 0.9$, $\beta_2 = 0.999$, a decay rate of 0.0, and $\epsilon = 1 \times 10^{-8}$, ensuring stable optimization throughout the training process. The total training duration was approximately 667.81 minutes, which is equivalent to about 11.13 hours.

Fig. 1 Bossbase database

$$ELU(x) = \begin{cases} x & \text{if } x > 0 \\ \alpha(e^x - 1) & \text{if } x \leq 0 \end{cases} \quad (1)$$

$$3\text{TanH} = 3x\frac{e^x - e^{-x}}{e^x + e^{-x}} \quad (2)$$

ELU (1) is used in one branch of the bifurcated CNN to improve gradient flow and enable faster, more stable training by reducing the vanishing gradient problem. It outputs the input directly when positive and smoothly approaches a negative value for negative inputs, controlled by the parameter alpha. The Tanh function amplifies the input before applying the tanh transformation, allowing the network to emphasize subtle variations in the data. In the proposed architecture, Tanh3 (2) is used in the second branch of the bifurcated CNN to increase non-linearity and enhance sensitivity to different feature patterns.

The formal mathematical representation of the 19-bit chromosome key is provided below to clarify its computational structure within the extraction process.
Formal Definition of the 19-bit Chromosome:

$$C=(c_1,c_2,\ldots,c_{19}) \in \{0,1\}^{19} \quad (3)$$

where the bit Equation 3 segments correspond to:

- **X coordinate (8 bits):** $(c_1, c_2, \ldots, c_8)$
- **Y coordinate (8 bits):** $(c_9, c_{10}, \ldots, c_{16})$
- **Inversion bit:** c_{17}
- **Direction bit:** c_{18}
- **Decompression bit:** c_{19}

The bifurcated CNN architecture is specified layer by layer to support reproducibility. Each input image is first processed through the 30 SRM filters which produce a 30 channel residual map. This residual tensor is then fed into two parallel convolutional branches. In the first branch, the residual input passes through three convolutional layers with filter sizes 3×3 and channel depths of 32, 64, and 128. Each layer is followed by batch normalization and ELU activation. The second branch mirrors this structure but replaces ELU with the Tanh3 activation function. Both branches apply global average pooling and the resulting feature vectors are concatenated into a single fused representation which is forwarded into two fully connected layers and a final softmax classifier. This explicit specification clarifies the bifurcation mechanism and the fusion process that leads to the improved representational capacity of the model.

5.3.01.bmp **4.2.04-2.bmp** **Testpat.bmp**

Fig. 2 Bows 2 database

Size : 16,838 bytes
Dimensions : 256×128
MD5 Hash :
f48b44a14ac223a5b3dac202f0fe759c

Cameraman.png

Fig. 3 Secret data

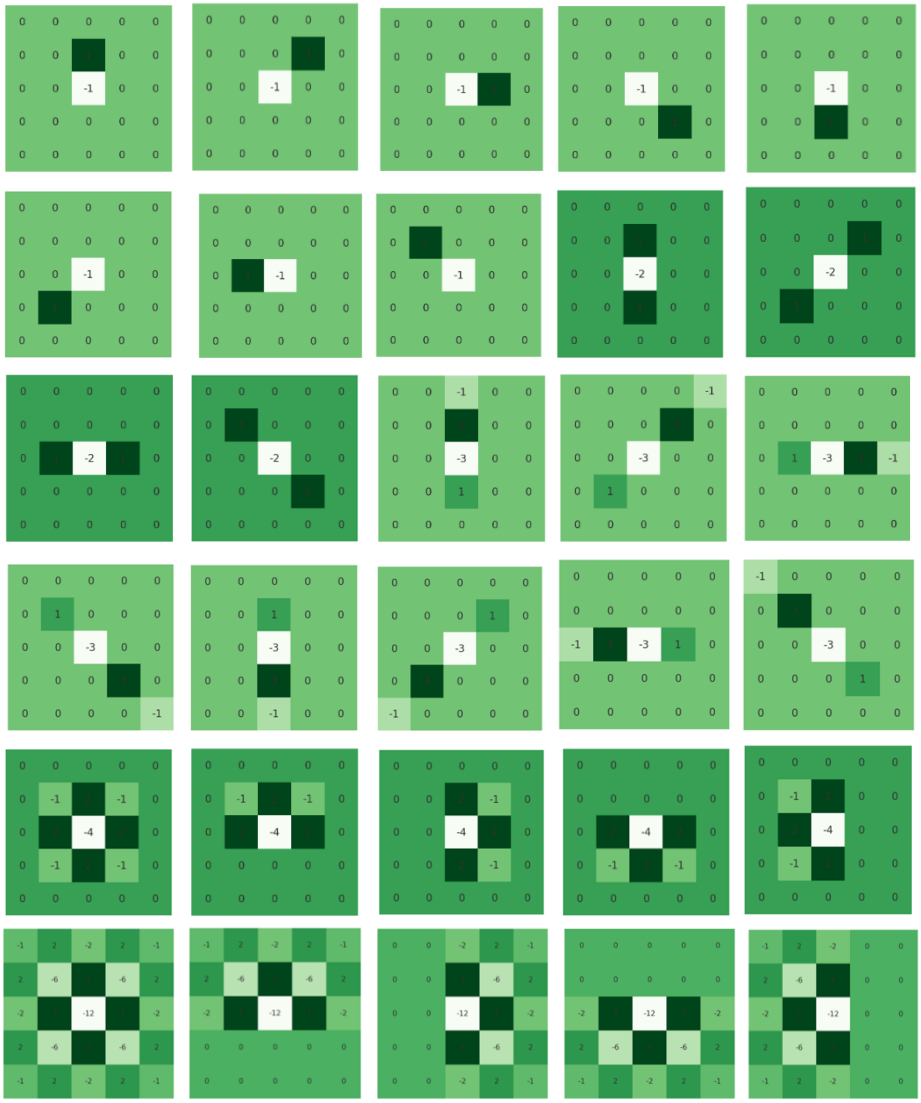

Fig. 4 30 SRM

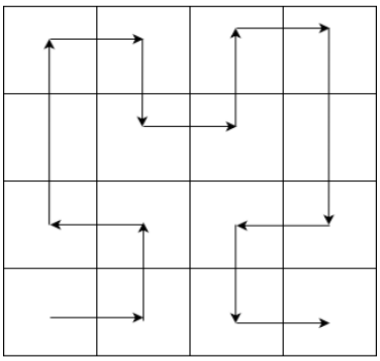

Fig. 5 4x4 Hilbert Curve

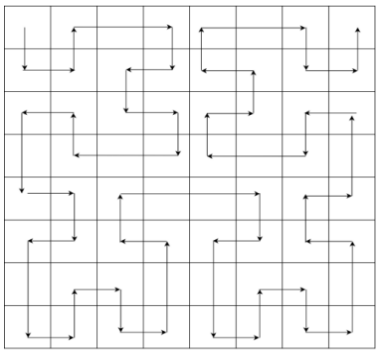

Fig. 6 8x8 Hilbert Curve

TABLE II
THE 19 BIT OF CHROMOSOME KEY

X Value	Y Value	Inversion	Direction	Decompression
8 Bit	8 Bit	1 Bit	1 Bit	1 Bit
0101 0101	1010 1010	0	1	0

Recent CNN-based steganalysis models including SRNet, Zhu-Net, and GBRAS-Net have shown strong performance in spatial-domain detection. However, these architectures typically rely on a single convolutional stream after SRM preprocessing and use activation functions that are largely homogeneous across layers. This design works reasonably well for conventional embedding schemes but becomes less effective when the hidden payload is produced by adaptive or evolutionary approaches such as the Genetic Algorithm based method used in this study. These modern approaches introduce diverse and shifting noise patterns that are not well captured by a single representational pathway. The proposed model introduces a bifurcated CNN architecture that deliberately separates the learning process into two distinct and complementary branches. This approach moves beyond the single-path structure of GBRAS-Net and also differs from the parallel modules used in ReST-Net. In ReST-Net [24] parallel branches primarily

diversify activation responses within a shared feature space. In contrast, the two branches in our design are constructed to perform different functional roles in analyzing residual noise.

The first branch uses ELU activation. This branch is effective at capturing low magnitude distortions because ELU improves gradient stability and remains sensitive to subtle residual noise that often arises when adaptive algorithms minimize detectable changes. The second branch uses Tanh3 activation, which applies a stronger non-linear transformation. This property makes the branch more responsive to irregular or abrupt distortions that may be introduced by more aggressive embedding decisions during the GA process. Taken together, these branches form two complementary feature subspaces. The ELU branch focuses on smooth and weak perturbations while the Tanh3 branch emphasizes sharper deviations from natural texture. The fused representation provides a richer and more discriminative feature manifold compared to single-stream architectures or parallel CNNs that do not explicitly differentiate their functional objectives. Another key novelty lies in the integration of the bifurcated detector with a complete payload extraction mechanism. Existing CNN-based steganalysis models focus solely on classification and do not provide a direct pathway for reconstructing the embedded message. The proposed framework is designed for forensic use, where both detection and recovery are essential. To our knowledge, this is the first architecture that combines dual-path feature extraction with genetic encoding and Hilbert Curve based spatial reordering in a single system capable of both identifying and reconstructing hidden payloads.

III. RESULT AND DISCUSSION

The proposed bifurcated GBRAS-Net model was evaluated on the BOSSbase 1.01 and BOWS 2 datasets using the experimental setup described in Section 3. The results show that the bifurcation-enhanced architecture consistently outperforms both the original GBRAS-Net and other established steganalysis models. As presented in TABLE II, the model achieved an average detection accuracy of **92.53%**, marking an improvement of approximately 4% over the baseline GBRAS-Net (89.8%). The improvement was consistent across both datasets, with accuracies of 93.25% on Image Fig. 1 and 92.40% on Imageb Fig. 2.

Against traditional statistical approaches such as Chi-Square and RS-Analysis, the advantage was even more pronounced. TABLE IV C shows that RS-Analysis reached only 2.6% detection accuracy, while Chi-Square barely exceeded 0.1% when faced with payloads embedded via adaptive genetic algorithm techniques. These results confirm that conventional statistical methods are ineffective against modern antiforensic strategies, whereas the proposed bifurcated CNN sustains high performance. A paired *t*-test confirmed that improvements over other deep learning baselines were statistically significant ($p < 0.01$).

Beyond classification accuracy, the extraction module also demonstrated exceptional robustness. Leveraging Hilbert Curve scrambling, genetic algorithm-based positioning, and LZMA decompression, the method reconstructed embedded messages in their entirety with zero data loss. As indicated in Fig. 7, the recovered payload matched the original both in size (16,838 bytes) and in MD5 hash value, confirming perfect recovery. This capability represents a key advantage over prior CNN-based steganalysis approaches such as SRNet [21] and Zhu-Net [25], which focus solely on detection without content reconstruction. TABLE III illustrates the superiority of the bifurcated CNN in detection accuracy, while the confusion matrix in TABLE IV shows a reduced false negative rate and low false positives, ensuring reliable classification without mislabeling cover images.

From a forensic perspective, the dual-stage design delivers two critical benefits. First, the enhanced detection accuracy ensures that covert communications embedded through adaptive steganography are reliably identified. Second, the payload recovery capability transforms steganalysis from a diagnostic tool into a reconstructive forensic instrument, enabling investigators to access the actual hidden content for evidentiary and intelligence purposes. This dual functionality directly addresses a major gap in current forensic workflows, where detection without recovery limits evidentiary value.

These findings also reaffirm the limitations of traditional statistical techniques, which perform poorly in adaptive antiforensic scenarios, with detection rates below 3%. The statistically significant improvement over other CNN architectures highlights the potential of bifurcated designs in capturing diverse noise patterns, making them a promising direction for future steganalysis research. Furthermore, the integration of genetic encoding, Hilbert Curve scrambling, and LZMA compression has proven effective in countering spatial distortion and redundancy in embedded data.

A. Ablation Study

An ablation study is an evaluation approach used to measure the contribution of each component in a model by deactivating or removing the component separately. When one component is turned off, the model's

performance is re-evaluated to see what changes occur. In this way, the study can empirically show which components have a significant impact on performance improvement and which components serve as supporting elements. This approach is commonly used in deep learning-based research because it provides clear evidence of the effectiveness of architectural designs and additional mechanisms introduced in the model.

An ablation study was conducted in this research to ensure that each proposed component truly contributes measurably to system performance. The model has three main elements, namely bifurcation architecture, genetic encoding mechanisms, and Hilbert Curve scrambling. All three work together in the full system, but their respective contributions need to be tested separately to ensure that performance improvements do not occur by chance or originate from only one particular component. By deactivating one component at a time and then re-evaluating its performance, this study was able to demonstrate a stronger causal relationship between the architectural design and the results obtained. This approach helped to ensure that the improvements in detection accuracy and payload reconstruction success did indeed stem from the interaction of the three proposed components.

An ablation study was conducted to evaluate the individual contributions of three key components in the proposed framework. These components are the bifurcated CNN architecture, the chromosome based genetic encoding, and the Hilbert Curve scrambling used to preserve spatial locality during payload reconstruction. The study isolates the effect of each component by selectively enabling or disabling it.

B. Findings

1) Impact of the bifurcated architecture: Both single-branch variants perform better than the baseline GBRAS-Net, indicating that each activation function contributes to improved sensitivity. The full bifurcation gives the highest accuracy among the detection-only variants, demonstrating that the two branches capture different aspects of the noise pattern and complement each other.

2) Impact of genetic encoding: Without chromosome based encoding, the extraction stage has no structural information about how the payload was embedded. Recovery becomes unreliable and incomplete. Genetic encoding provides a structured search space that significantly improves reconstruction performance even before spatial reordering is applied.

TABLE III
PRIOR METHOD COMPARISON

Nama Metode	Accuracy
Xu Net [14]	79.3
Ya Net [26]	76.7
Yedroudj Net [27]	85.1
SRNet s[21]	86.4
Zhu-Net [25]	88.1
GBRAS-Net [23]	89.8
GBRAS-Net Bifurcated	92.53

TABLE IV
DETECTION RESULT OF PRIOR RESEARCH

File Name	Stego/ Cover	Detection Result	Steganalysis with Chi Square	Steganalysis with RS Analysis	Steganalysis with Fusion (Mean)
4.2.03GA.bmp	Stego	FALSE	0.0008	0.1028	0.0630
4.2.04GA.bmp	Stego	FALSE	0.0013	0.0223	0.0229
4.2.05GA.bmp	Stego	FALSE	0.0045	0.0260	0.0221
4.2.06GA.bmp	Stego	FALSE	0.0000	0.0238	0.0162
4.2.07GA.bmp	Stego	FALSE	0.0000	0.0082	0.0083

Fig. 7 Result of extraction

TABLE V
ABLATION STUDY OF KEY COMPONENTS

Model Variant	Bifurcation	Genetic Encoding	Hilbert Curve	Detection Accuracy	Payload Recovery
Baseline GBRAS-Net	No	No	No	89.8%	Not applicable
Single branch ELU only	Yes	No	No	Higher than baseline	Not applicable
Single branch Tanh3 only	Yes	No	No	Higher than baseline	Not applicable
Full Bifurcation	Yes	No	No	92.53%	Not applicable
Bifurcation plus GA Encoding	Yes	Yes	No	92.53%	Partial recovery
Full Model	Yes	Yes	Yes	92.53%	100 percent recovery

3) Impact of Hilbert Curve scrambling: Hilbert traversal restores the correct neighborhood relationships among pixels. This step is essential for removing redundancy and enabling accurate decompression. Once this component is added, the system achieves perfect payload recovery with matching MD5 hashes.

The ablation results confirm that the performance of the system is not due to a single architectural element. Instead, each component plays a distinct role and the overall improvement arises from the interaction between complementary feature extraction, structured embedding parameter recovery, and spatial preservation during reconstruction.

The proposed framework can be integrated into forensic operations in a practical and direct manner. In a laboratory setting, the bifurcated detection stage can be embedded into existing triage tools or custom preprocessing pipelines to automatically screen large collections of images during evidence intake. Because the model performs inference with low latency, it can operate on batches of files without delaying standard acquisition or examination workflows. This enables early identification of suspicious images and allows investigators to prioritize items that may contain hidden communication. The extraction component can then be linked to evidence management systems so that recovered payloads, together with integrity information such as MD5 values, are logged automatically within the chain of custody. This provides investigators with not only the detection result but also a reproducible record of the recovered data which can support analysis, attribution, or courtroom presentation. The model can also be compiled as a standalone command line utility or as a plug in for existing forensic suites since its computational footprint is small enough to run on typical workstation hardware used by law enforcement and forensic laboratories.

From an operational perspective, the framework is well suited for agencies that routinely encounter concealed communication channels, such as law enforcement units, cybersecurity teams, and intelligence organizations. Reliable detection reduces the likelihood

that covert channels remain unnoticed during digital evidence handling, while the ability to reconstruct payloads allows the recovery of critical information that may contain planning data, exchange of signals, or embedded documents relevant to a case. These characteristics position the system as more than a classification tool and closer to a practical forensic instrument that supports both investigative and evidentiary needs.

Despite these advantages, several limitations remain. The current experiments focus solely on grayscale images and do not address the complexities introduced by color imagery, where noise characteristics differ across channels and require multichannel residual extraction. The model also exhibits reduced robustness under aggressive compression, geometric distortion, and noise injection. In addition, although inference is efficient, the genetic algorithm used during payload recovery introduces computational overhead during the search for optimal extraction parameters, which may affect throughput in large scale workflows.

Future research will address these limitations in several ways. Extending the framework to color images will require color aware SRM filters and branch specific feature extraction strategies designed for multichannel inputs. Improving computational efficiency will involve pruning and quantization methods, mixed precision training, and restructuring parts of the extraction pipeline to reduce the search space of the genetic algorithm. Finally, the system will be evaluated within complete forensic pipelines that include ingestion, triage, detection, extraction, and reporting. This includes developing interfaces for popular forensic tools and validating performance under operational constraints to ensure that the framework remains reliable, scalable, and adaptable to the diverse conditions encountered in real world digital investigations.

IV. CONCLUSION

This study presented a dual stage steganalysis framework that combines a bifurcated CNN architecture with a genetic algorithm based payload extraction module. The bifurcated design enhances the representational capacity of GBRAS-Net by allowing two complementary feature learning paths that respond differently to subtle and non linear noise patterns. The extraction module, which integrates chromosome based encoding, Hilbert Curve traversal, and LZMA decompression, enables complete and lossless payload reconstruction. Experiments on the BOSSBase 1.01 and BOWS2 datasets show that the framework achieves higher detection accuracy than established CNN based steganalysis models and delivers perfect payload recovery, demonstrating its utility for forensic applications. Beyond technical performance, the framework is suitable for practical deployment in digital forensic workflows. The detection stage can serve as an automated screening component in triage systems or preprocessing pipelines, while the extraction stage can integrate with evidence handling platforms to produce verifiable recovered payloads supported by integrity metadata. These capabilities strengthen the evidentiary value of hidden content and support investigative processes in law enforcement, cybersecurity operations, and intelligence analysis. Several limitations remain. The current system focuses on grayscale images and has not yet been extended to color imagery or other media formats, where noise behavior varies across channels. The model shows sensitivity to heavy compression and geometric distortions, and the genetic algorithm introduces computational overhead that may affect large scale or time critical deployments. These challenges highlight the need for additional optimization and broader evaluation. The future work will address these limitations by incorporating multichannel residual extraction for color images, adopting model optimization techniques such as pruning, quantization, and mixed precision training, and evaluating robustness under diverse media conditions including compressed or perturbed imagery. The framework will also be developed into a fully automated forensic pipeline that supports ingestion, triage, detection, extraction, and reporting, followed by validation in operational environments to ensure reliability and forensic readiness. This research was conducted entirely using public benchmark datasets without involving personal data or human subjects, and therefore complies with ethical standards in forensic computing research. Overall, the proposed framework offers a robust and practical approach to modern steganalysis and establishes a solid foundation for future advancements in adaptive antiforensic countermeasures and forensic evidence reconstruction.

ACKNOWLEDGEMENT

This study does not involve human subjects, personal data, or any privacy-sensitive information. All experiments were conducted using publicly available benchmark datasets, specifically BOSSBase 1.01 and BOWS2, which contain non-identifiable grayscale images commonly used in steganalysis research. No real forensic case data, confidential material, or user-generated content were accessed during the study. The work therefore complies with standard ethical practices

in forensic computing research and does not require institutional review or additional ethical clearance. This publication is part of a research project funded by the Directorate of Research, Technology, and Community Service – Directorate General of Higher Education, Research, and Technology (Diktiristek), Ministry of Education, Culture, Research, and Technology of the Republic of Indonesia, through the Thesis Research Grant scheme for Fiscal Year 2025, under Contract Number: 0498.01/LL5-INT/AL.04/2025. The authors gratefully acknowledge the financial support provided, which played a significant role in the successful implementation of this research.

REFERENCES

[1] N. Hidayasari, I. Riadi, and Y. Prayudi, "Steganalisis Blind dengan Metode Convolutional Neural Network (CNN) Yedroudj- Net terhadap Tools Steganografi," *Jurnal Teknologi Informasi dan Ilmu Komputer*, vol. 7, no. 4, pp. 787–796, Aug. 2020, doi: 10.25126/jtiik.2020703326.

[2] P. K. Madi and Y. Prayudi, "Analisis Kualitas Audio Steganografi MP3 Menggunakan Teknik Masking Pada Spectrogram," *Jurnal Sains, Nalar, dan Aplikasi Teknologi Informasi*, vol. 4, no. 2, pp. 138–148, Jul. 2025, doi: 10.20885/snati.v4.i2.40248.

[3] Z. Guo, "Regulating the use of electronic evidence in Chinese courts: Legislative efforts, academic debates and practical applications," *Computer Law & Security Review*, vol. 48, p. 105774, Apr. 2023, doi: 10.1016/j.clsr.2022.105774.

[4] S. Chen, C. Zhao, L. Huang, J. Yuan, and M. Liu, "Study and implementation on the application of blockchain in electronic evidence generation," *Forensic Science International: Digital Investigation*, vol. 35, p. 301001, Dec. 2020, doi: 10.1016/j.fsidi.2020.301001.

[5] B. Halopeau, "Terrorist use of the internet," in *Cyber Crime and Cyber Terrorism Investigator's Handbook*, Elsevier, 2014, pp. 123–132. doi: 10.1016/B978-0-12-800743-3.00010-4.

[6] M. Salman and A. Uhl, "Countering Anti-forensics of SIFT-based Copy-Move Detection," in *2020 25th International Conference on Pattern Recognition (ICPR)*, IEEE, Jan. 2021, pp. 2701–2707. doi: 10.1109/ICPR48806.2021.9413012.

[7] K. Uddin, Y. Yang, and B. T. Oh, "Deep learning-based counter anti-forensic of GAN-based attack in HEVC compressed domain using coding pattern analysis," *Expert Syst. Appl.*, vol. 233, p. 120912, Dec. 2023, doi: 10.1016/j.eswa.2023.120912.

[8] J. Fridrich and M. Goljan, "<title>Practical steganalysis of digital images: state of the art</title>," E. J. Delp III and P. W. Wong, Eds., Apr. 2002, pp. 1–13. doi: 10.1117/12.465263.

[9] J. Fridrich, M. Goljan, and R. Du, "Reliable detection of LSB steganography in color and grayscale images," in *Proceedings of the 2001 workshop on Multimedia and security new challenges - MM&Sec '01*, New York, New York, USA: ACM Press, 2001, p. 27. doi: 10.1145/1232454.1232466.

[10] S. Wu, S. Zhong, and Y. Liu, "A Novel Convolutional Neural Network for Image Steganalysis With Shared Normalization," *IEEE Trans. Multimedia*, vol. 22, no. 1, pp. 256–270, Jan. 2020, doi: 10.1109/TMM.2019.2920605.

[11] J. Ye, J. Ni, and Y. Yi, "Deep Learning Hierarchical Representations for Image Steganalysis," *IEEE Transactions on Information Forensics and Security*, vol. 12, no. 11, pp. 2545–2557, Nov. 2017, doi: 10.1109/TIFS.2017.2710946.

[12] A. P. Purnacandra and S. Subektiningsih, "Anti-Forensics with Steganographic File Embedding in Digital Image Using Genetic Algorithm," *Jurnal Ilmiah Teknik Elektro Komputer dan Informatika*, vol. 8, no. 2, p. 326, Jul. 2022, doi: 10.26555/jiteki.v8i2.24208.

[13] Y. Qian, J. Dong, W. Wang, and T. Tan, "Deep learning for steganalysis via convolutional neural networks," A. M. Alattar, N. D. Memon, and C. D. Heitzenrater, Eds., Mar. 2015, p. 94090J. doi: 10.1117/12.2083479.

[14] G. Xu, H.-Z. Wu, and Y.-Q. Shi, "Structural Design of Convolutional Neural Networks for Steganalysis," *IEEE Signal Process. Lett.*, vol. 23, no. 5, pp. 708–712, May 2016, doi: 10.1109/LSP.2016.2548421.

[15] L. Jia, A. Gao, M. Li, X. Fu, H. Zhou, and J. Ding, "HMSNet: Hilbert curve enhanced Mamba for real-time semantic segmentation," *Pattern Recognit.*, vol. 172, p. 112457, Apr. 2026, doi: 10.1016/j.patcog.2025.112457.

[16] E. J. Leavline, D. Asir, and A. G. Singh, "ISSN : 2249-0868 Foundation of Computer Science FCS," 2013. [Online]. Available: www.ijais.org

[17] A. Dwaik and Y. Belkhouche, "Enhancing the performance of convolutional neural network image-based steganalysis in spatial domain using Spatial Rich Model and 2D Gabor filters," *Journal of Information Security and Applications*, vol. 85, p. 103864, Sep. 2024, doi: 10.1016/j.jisa.2024.103864.

[18] M. Gao and P. Qian, "Exponential linear units-guided Depthwise separable convolution network with cross attention mechanism for hyperspectral image classification," *Signal Processing*, vol. 210, p. 108995, Sep. 2023, doi: 10.1016/j.sigpro.2023.108995.

[19] P. Bas, T. Filler, and T. Pevný, ""Break Our Steganographic System": The Ins and Outs of Organizing BOSS," 2011, pp. 59–70. doi: 10.1007/978-3-642-24178-9_5.

[20] S. Manoharan, "An Empirical Analysis of RS Steganalysis," in *2008 The Third International Conference on Internet Monitoring and Protection*, IEEE, 2008, pp. 172–177. doi: 10.1109/ICIMP.2008.15.

[21] M. Boroumand, M. Chen, and J. Fridrich, "Deep Residual Network for Steganalysis of Digital Images," *IEEE Transactions on Information Forensics and Security*, vol. 14, no. 5, pp. 1181–1193, May 2019, doi: 10.1109/TIFS.2018.2871749.

[22] X. Shi, B. Tondi, B. Li, and M. Barni, "CNN-based steganalysis and parametric adversarial embedding:A game-theoretic framework," *Signal Process. Image Commun.*, vol. 89, p. 115992, Nov. 2020, doi: 10.1016/j.image.2020.115992.

[23] T.-S. Reinel, "GBRAS-Net: A Convolutional Neural Network Architecture for Spatial Image Steganalysis," *IEEE Access*, vol. 9, pp. 14340–14350, 2021, doi: 10.1109/ACCESS.2021.3052494.

[24] B. Li, W. Wei, A. Ferreira, and S. Tan, "ReST-Net: Diverse Activation Modules and Parallel Subnets-Based CNN for Spatial Image Steganalysis," *IEEE Signal Process. Lett.*, vol. 25, no. 5, pp. 650–654, May 2018, doi: 10.1109/LSP.2018.2816569.

[25] R. Zhang, F. Zhu, J. Liu, and G. Liu, "Depth-Wise Separable Convolutions and Multi-Level Pooling for an Efficient Spatial CNN-Based Steganalysis," *IEEE Transactions on Information Forensics and Security*, vol. 15, pp. 1138–1150, 2020, doi: 10.1109/TIFS.2019.2936913.

[26] J. Ye, J. Ni, and Y. Yi, "Deep Learning Hierarchical Representations for Image Steganalysis," *IEEE Transactions on Information Forensics and Security*, vol. 12, no. 11, pp. 2545–2557, Nov. 2017, doi: 10.1109/TIFS.2017.2710946.

[27] M. Yedroudj, F. Comby, and M. Chaumont, "Yedroudj-Net: An Efficient CNN for Spatial Steganalysis," in *2018 IEEE International Conference on Acoustics, Speech and Signal Processing (ICASSP)*, IEEE, Apr. 2018, pp. 2092–2096. doi: 10.1109/ICASSP.2018.8461438.